Journal of New Materials for Electrochemical Systems 13, 127-131 (2010)

Photoelectrocatalysis with Drop-Cast Tungsten Trioxide Films

M. Neumann-Spallart* and S. B. Sadale

Groupe d'Étude de la Matière Condensée, C.N.R.S., 1, place Aristide Briand, 92195 Meudon CEDEX, France.

Received: Nobember 23, 2009, Accepted: June 09, 2010

Abstract: *Polycrystalline, monoclinic, uniform WO_3 films of up to 2.5 µm thickness were prepared by drop casting onto F:SnO_2/glass using as precursor peroxo-tungstic acid and polyethylene glycol in water, and firing in air at 520°C.*

Under illumination of such n-type semiconducting electrodes in junctions with aqueous electrolytes, photocurrents were produced. Under depletion conditions, IPCEs (incident photon to current efficiencies) of up to 0.7 at 365 nm and 0.2 at 405 nm were obtained. The photosensitivity extends into the visible with an onset at 470 nm. This opens the way for solar light powered electrochemical processes like pollutant degradation.

The photocatalytic activity of such layers was examined using the azo-dye acid orange 7 (AO7) as a model pollutant. Degradation of 1 mM AO7 was carried out under backside UVA broadband illumination of electrodes of 62 cm^2 active surface area, using a thin film flow-through reactor equipped with a stainless steel counter electrode, rapid recirculation of the electrolyte, and electrical bias of 1.1 - 1.3 V. During illumination, the concentration of AO7 decreased with an apparent first order rate constant, k, of $1.44 \cdot 10^{-4}$ s^{-1}, corresponding to a specific decay constant of $2.3 \cdot 10^{-7}$ $l \cdot s^{-1} \cdot cm^{-2}$ for a light intensity of $4.7 \cdot 10^{-9}$ $E \cdot s^{-1} cm^{-2}$.

Keywords: photoelectrocatalysis, WO_3, acid orange 7

1. INTRODUCTION

In the search for photocatalysts with extended visible light photosensitivity, tungsten trioxide turns out to be an interesting candidate. WO_3 is an n-type semiconductor with an indirect bandgap of 2.7 eV [1], and for polycrystalline material (thin films) a value of 2.6 eV has been measured at room temperature [2]. A conduction band position of around 0.5 V vs. NHE has been reported for pH 2 [3]. For polycrystalline materials, flatband potentials depend to a large extent on the way of preparation [4]. WO_3 is chemically stable in acid solution and cannot be oxidized [5].

Recently, the photodegradation of oxalic acid on WO_3 electrodes under electrical bias was reported [6]. Photocatalysis with transition metal oxides is a process based on their semiconducting nature [7] and junction behaviour can therefore be influenced by electrical bias if the material is immobilized in the form of a macroscopic electrode. Application of electrical bias in photocatalysis with immobilized semiconductors was shown to increase the efficiency of the process considerably [6], as charge carrier recombination in the bulk of the semiconductor is suppressed. For n-type semiconductors, there are cases where oxidative photodegradation does not take place at all in the absence of bias, as for instance for WO_3 electrodes of a similar type as used in this work, and a test molecule, the azo-dye acid orange 7 (4-(2-hydroxy-1-naphthylazo)benzenesulfonic acid sodium salt, AO7) [8]. This was ascribed to the lack of a complementary reduction process (oxygen reduction) on the surface of the semiconductor, in contrast to what is observed with most TiO_2 catalysts.

Several chemical methods for WO_3 thin film deposition have been used, *viz.* spray pyrolysis, electrodeposition [9], brush painting, dip- and spin-coating. In spray pyrolysis, aqueous solvents tend to give strongly light scattering [10] and sometimes powdery deposits. If organic solvents are to be used, organometallic precursors have to be employed which are expensive and sensitive to humidity. In discontinuous (layer by layer) growth methods (brush painting [2], dip coating, and spin coating [2]), many application/annealing cycles are needed to build up a thick film and each of the annealing step needs slow heating-up / cooling-down in order to avoid breakage of large samples. Moreover, the total annealing time has an influence on the doping by oxygen vacancies. Especially in the case of WO_3 it has been shown that prolonged annealing at > 500°C leads to overdoping due to irreversible oxygen loss. Mesoporous WO_3 has been deposited from tungstic acid

*To whom correspondence should be addressed: Email: mns@cnrs-bellevue.fr

with a large amount of organic stabilizer in the precursor solution [11].

In this study we report on the preparation of WO_3 films by drop casting, using a new precursor (peroxotungstic acid / polyethylene glycol). Peroxotungstic acid has recently been used for aerosol pyrolysis deposition of WO_3 [10]. The addition of polyethylene glycol increases the viscosity of the precursor solution of which a thicker layer can be spread on the surface to be coated.

We further report on the photoelectrochemical properties of such electrodes, and their use (in the form of large area electrodes) in a photo-electrocatalytic process in view of water purification using solar light. As an oxidatively degradable test molecule for the activity of the photocatalyst, AO7 was used, as its concentration can be easily monitored due to its high extinction coefficient. Another azo-dye, Remazol Black B [12], has recently been shown to be photodegraded on illuminated WO_3 obtained by electrodeposition and annealing. There is some interest in the degradation of AO7 itself, because it is a commonly used textile dye, and due to its structure, representative for a whole class of compounds.

A flow-through photoelectrochemical cell as described in [13] accommodating 10 cm x 10 cm electrodes was used for the study of solute degradation.

2. EXPERIMENTAL

2.1. Sample preparation and physical characterisation.

F-doped SnO_2 coated glass plates with surface resistivities between 9 and 28 Ω were used as substrates, which were cleaned ultrasonically in trichlorethylene, acetone, ethanol and water, followed by etching in 5% HF for 1 min., water rinsing and drying with a stream of argon.

Aqueous solutions of peroxotungstic acid were prepared by adding 2.49 g of H_2WO_4 to 50 ml of 15% H_2O_2. A clear solution was obtained after constant stirring for 48 h. This solution was further diluted with distilled water. The precursor solution was prepared by mixing this solution with polyethylene glycol (PEG300). The final precursor solution was 0.075 M peroxo-tungstic acid and 25% v/v PEG300 in water. All chemicals were of analytical grade and used without further purification. Water was purified with a Millipore apparatus.

Small electrodes (1 cm x 5 cm) were prepared by one to five cycles of casting (spreading) of a liquid film onto the substrates, air drying and annealing in air. Large electrodes (10 cm x 10 cm) were prepared by a single casting – drying – annealing cycle using different amounts of precursor solution for preparing films of different thickness. Scotch tape, extending above the surface to be coated was attached to the borders of the substrate plates which were kept as horizontal as possible. The precursor solution was then poured into this trough followed by drying in air at room temperature and, finally, annealing in air.

X-ray diffraction (XRD) measurements were carried out with a Philips PW1710 diffractometer using Cu-K_α radiation. The thickness of the SnO_2 coating and of the WO_3 films deposited on it was estimated from the interference patterns measured using a fiber optic spectrometer in reflection mode and the program Nanocalc (Mikropack, Germany). Large electrodes were mapped as to thickness.

2.2. Electrochemical characterisation.

Photoelectrochemical tests were performed using either a potentiostatic set-up where potentials are quoted vs. a saturated calomel electrode (SCE), or, in the case of large electrochemical cells, a two terminal configuration were the voltage difference (bias) between the two electrodes is given. For testing of small electrodes (1 cm x 5 cm), a 150 W medium pressure mercury lamp in combination with 365 nm and 313 nm band-pass filters was used for illumination. In addition, LEDs with centre wavelengths of 376.9 nm and 403.11 nm were used. At these wavelengths, the photocurrents generated by the sample or those generated by a calibrated Hamamatsu 1337-1010BQ photodiode under potentiostatic control were measured. External quantum yields of charge collection (IPCE, based on the number of incident photons) were calculated from these data.

Large electrodes (10 cm x 10 cm) were mapped as to IPCE by collecting data from 9 areas of 0.5 cm^2 distributed over the surface using backside irradiation (through the transparent substrate) with an LED emitting at 403.11 nm.

2.3. Photoelectrocatalytic degradation.

Solute degradation experiments were carried out in a thin film flow-through electrochemical cell with a stainless steel counter electrode at a distance of 1 mm and rapid recirculation of the electrolyte. An active electrode surface area of 62 cm^2 was exposed to the electrolyte and to backside illumination (through the transparent conducting substrate), using a "black-light" 15 W UVA broadband lamp (Conrad) with a centre wavelength of 365 nm. Based on the spectral emission characteristics and the mean IPCE obtained from mapping, the mean light intensity at the location of the film was estimated to be $4.7 \cdot 10^{-9}$ $E \cdot s^{-1} \cdot cm^{-2}$. The total organic carbon content (TOC) was measured with a Shimadzu autosampling TOC analyzer employing a non-dispersive infra-red detector.

3. RESULTS AND DICUSSION

Deposits for photoelectrochemical characterisation and utilization in a photoelectrochemical reactor require an electrically conducting substrate. Therefore, WO_3 films were prepared on F:SnO_2/glass substrates. In combination with the water soluble WO_3 precursor, peroxotungstic acid, PEG300 was used in order to increase the viscosity of the precursor solution and to allow for crack-free drying. Several cast – dry – anneal cycles were performed in order to obtain up to 2.5 μm thick, well adherent films on small substrates. The films were polycrystalline and monoclinic as shown by the X-ray diffraction diagram (Fig. 1). They have a specular aspect, indicating low roughness. A cross section of a layer obtained by 5 cycles with intermediate annealing in air at 500°C and final annealing at 520°C is shown in Fig. 2. The scanning electron micrograph reveals a regular, somewhat porous film consisting of 50 nm diameter WO_3 grains on top of a dense SnO_2 layer supported on glass. This shows that the organic additive (PEG300) undergoes smooth decomposition upon firing. In contrast to dip coating, where only a very thin film adheres on the substrate upon withdrawal, with drop-casting where the substrate is kept horizontally, large amounts of precursor solution can be applied at once. As the precursor solution dried without precipitation of the precursor and no cracking upon drying and firing occurred, large electrodes were fabricated using a single application, suffic-

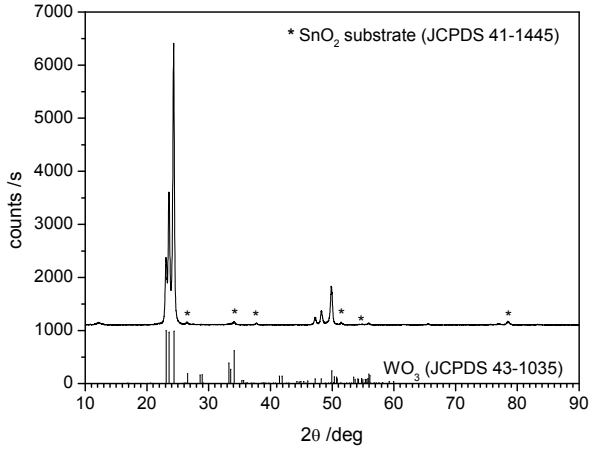

Figure 1. XRD of WO_3 film on F:SnO_2/glass. Substrate peaks (SnO_2 (cassiterite)) are marked with an asterisk. Standard diffraction pattern of WO_3 from ref. [15].

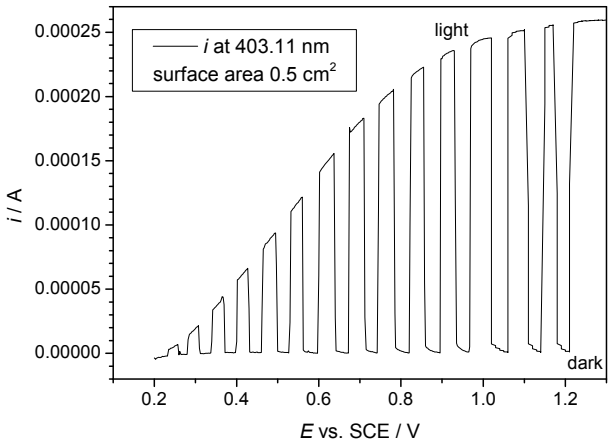

Figure 3. Current - potential curve under chopped backside illumination (403.11 nm). Electrolyte … 0.1 M air saturated $HClO_4$, scan rate 20 mV/s.

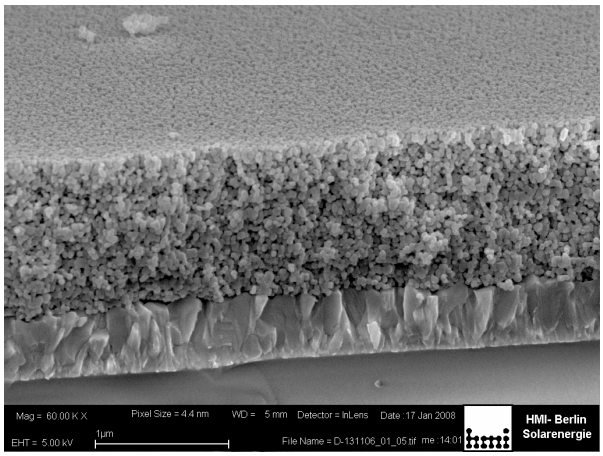

Figure 2. SEM picture of a cross section of a layer of WO_3 on F:SnO_2/glass.

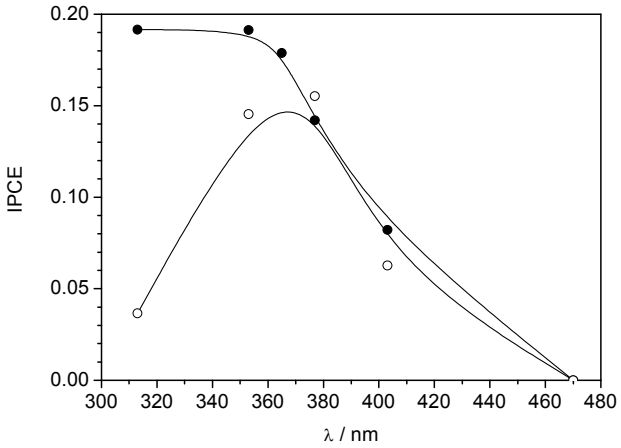

Figure 4. IPCE as a function of wavelength for EE and SE illumination. 0.1 M $HClO_4$, 1.2 V *vs*. SCE, filled circles … EE illumination, open circles … SE illumination.

ing to build up a thick film as required for absorbing a large part of the incident light.

3.1. Photoelectrochemical properties.

On the WO_3 electrodes in junctions with aqueous electrolytes, photocurrents consistent with the behaviour of an n-type semiconductor were produced upon both, front-side as well as backside illumination. As there is no oxidizable species present in the solution, and WO_3 is not oxidized by valence band holes, the photocurrents are entirely ascribed to water oxidation. A potentiodynamic scan in 0.1 M $HClO_4$, an electrolyte in which WO_3 is known to be stable, under rectangularly chopped monochromatic illumination shows that a photocurrent plateau is approached around 1 V *vs*. SCE (Fig. 3). Cathodic dark currents were negligible in potential regions where photocurrents flowed, in spite of the presence of oxygen being a potential depolarizer. This is the reason why under illumination without bias (conventional photocatalysis, "open circuit") a photopotential in a region where high photocurrents flow can not be established on this type of material and therefore no oxidation reaction of solutes can take place (see below). (Identical current – potential characteristics have been obtained with WO_3 electrodes fabricated by spray pyrolysis [7]). The onset of photocurrents occurred around 0.2 V *vs*. SCE. Polarizing the electrodes to potentials below that value was avoided in order to prevent alteration of the electrode due to hydrogen intercalation (leading to blue colouration - a process which is used in electrochromic applications).

The incident photon to current efficiency (IPCE) was measured a function of wavelength in 0.1 M $HClO_4$ under depletion conditions (in the potential region of plateau photo-currents, 1.2 V vs. SCE) (Fig. 4). The photosensitivity extends into the visible, with an onset around 470 nm in accordance with the bandgap of tungsten trioxide and the absorption spectrum of WO_3 thin films [2]. This opens the way for solar light driven electrochemical processes like oxidative pollutant degradation. With front-side illumination (EE), IPCE values tend towards a plateau value at low wavelengths. For thicker

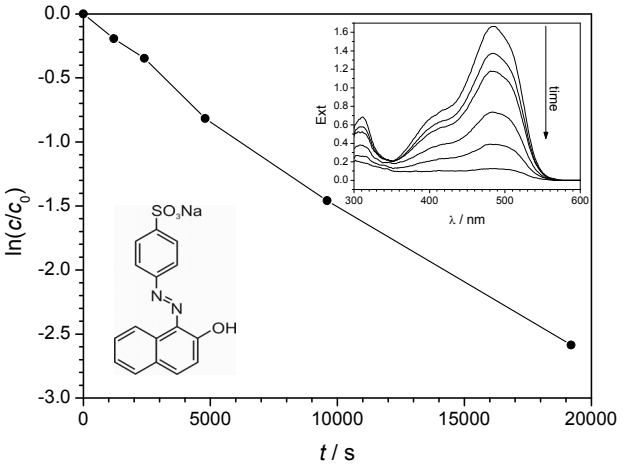

Figure 5. Degradation of 1 mM AO7 in 10 mM $HClO_4$ with UVA broadband illumination on WO_3. Electrical bias: 1.3 V vs. steel, flow velocity 35.7 cm·s^{-1}, total liquid volume 0.1 l. Lower left inset … structure of AO7, upper right inset … spectral changes of the solution as a function of time of irradiation. The extinction at 485 nm is taken as a measure for the AO7 concentration.

electrodes, values up to 0.7 were reached. With backside illumination (SE), photocurrents (and therefore IPCE) decrease at lower wavelength, due to the limited minority carrier diffusion length, and at very low wavelength due to light absorption by the transparent conductor, F:SnO_2/glass. The location of the ensuing wavelength for maximum IPCE therefore depends also on thickness, and for technical applications the thickness and the spectral output characteristics of the light source have to be matched. In the example given in Fig. 4, the layer thickness was optimized for polychromatic SE illumination (UVA black light lamp with a broad emission peak centred at 365 nm), and IPCE for SE reached 0.2 at 365 nm.

In large electrodes, the WO_3 thickness varied considerably over the 100 cm^2 surface area due to the single-step application of a large quantity of precursor solution. In a typical sample, a thickness of 1000 nm was found with a standard deviation of 390 nm, based on the measurement of 9 points. In spite of this fact, IPCE mapping at the same points using an LED (peak wavelength 403.11 nm, producing photocurrents of typically 150 µA from a surface of 0.5 cm^2) led to deviations from the mean IPCE (0.08) of only +/− 15%, indicating that the film was thick enough for absorbing a major part of the light at this wavelength. The mean IPCE was similar to that measured for small electrodes of comparable thickness.

3.2. Photoelectrocatalysis.

In photocatalysis on n-type semiconductors, solutes are oxidatively degraded by valence band holes generated by absorption of photons of energy higher than the bandgap of the semiconductor, or by products formed by these holes (e.g. OH radicals).

The photocatalytic activity of the WO_3 layers was examined using large electrodes (10 cm x 10 cm) obtained by a single casting cycle. 62 cm^2 of the electrodes were exposed to the electrolyte and light. A stainless steel counter electrode of identical form and surface area was kept at a distance of 1 mm. Such a small distance was selected in order to minimize ohmic drop when electrolytes of low conductivity (as an extreme one can think of tap water, 528 µS/cm at the location of the laboratory) were used. In this series of experiments, in order to maintain constant ionic strength and pH, 10 mM $HClO_4$ (3700 µS/cm, pH 2.68) was used as inert supporting electrolyte. The electrolyte (total volume of 0.1 l) was rapidly pumped through the cell using recirculation *via* an external reservoir. Between the WO_3 electrode and the counter electrode sufficient bias was applied to drive the potential of the WO_3 electrode to values where maximal photocurrents flow (1.1 to 1.3 V). The electrodes were backside illuminated (through the transparent substrate) using a UVA broadband source. As the light encounters the semiconductor layer first and is absorbed by it, direct photolysis of solutes can be minimized.

On electrodes of different thickness, during irradiation with a UVA lamp, photocurrents, i_{ph}, between 2 and 5 mA were produced in the plateau region using 10 mM $HClO_4$ as electrolyte. Addition of the azo-dye AO7 (structure shown as inset in Fig. 5) serving as a test substance for the photocatalytic activity of the catalyst layers did not increase the photocurrent. Optical absorption spectra of aliquots withdrawn from the reactant solution at various time intervals showed a steady decrease in extinction at all wavelengths. The extinction at 485 nm was taken as a measure for the concentration, c, of AO7 in the aqueous solution. In the experiment of which data are presented in Fig. 5, c (initial value 1 mM, TOC 192 mg/l) decreased with an apparent first order rate constant, k, of $1.44 \cdot 10^{-4}$ s^{-1}. In the absence of light or in the absence of bias, the decrease of the concentration was only 10 % after several hours of operation, whereas under illumination and bias concentrations were reduced by up to 97 % for similar durations. As the degradation rate is indirectly proportional to the total liquid volume, V, and proportional to the illuminated surface area (assuming a homogeneous irradiation field), a specific decay constant can be calculated from the kinetic data, which amounts to $2.3 \cdot 10^{-7}$ l·s^{-1}·cm^{-2} for an intensity of $4.7 \cdot 10^{-9}$ E·s^{-1}·cm^{-2}.

From the degradation curves, the Faradaic efficiency, $f = (V\mathrm{d}c/\mathrm{d}t)/(i_{ph}/\mathrm{F})$, can be calculated as a function of degradation time (and therefore concentration), where F is the Faraday (96500 C/mol). A Faradaic efficiency of around 30 percent was found for 1 mM AO7, whereas for 0.1 mM f drops below 5 percent. The remaining part of the photocurrent is used for the oxidation of the solvent, water.

The degradation rates and rate constants refer to the destruction of the main chromophore of AO7, resulting in the production of various smaller organic molecules in the solution. Preliminary TOC measurements show that the complete mineralization (decomposition into small inorganic molecules) of AO7 occurs at a much lower rate, with the rate limiting step being the destruction of the aromatic ring systems, as shown by UV-Vis absorption of the solution as a function of irradiation time.

3.3. Role of mass transport.

Measurements at various liquid flow velocities showed that the reaction rate depended on mass transport. In general, photoelectrochemical reactions rates at interfaces are controlled by both, mass transport and photon flux, depending on light intensity and flow velocity. It has been shown [2] that in single-pass flow-through

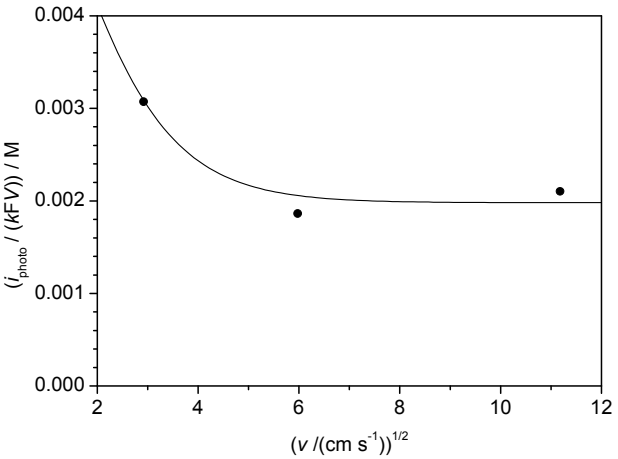

Figure 6. Influence of the mean liquid flow velocity on the photoelectrocatalytic degradation of 1 mM AO7 in 10 mM $HClO_4$ by UVA broadband illuminated WO_3. i_{ph} ... photocurrent, k ... observed decay constant, V ... total liquid volume.

mode, high conversion efficiency (low outlet concentrations) can be obtained, but at the expense of incomplete utilization of the incident photons, as the degradation rate would not increase when the intensity is increased. Alternatively, recirculation of a given volume in combination with high flow velocities can be used, thus minimizing rate limitation by mass transport (diffusion and convection). This approach has been used in the present study.

In order to abstract from the influence of the photocurrent on the degradation rates, a parameter, $s = i_{ph}/kFV$, can be calculated from the decay data (Fig. 5). (Note that s is defined such that a lower value corresponds to a higher catalytic activity). For a given photon flux, at high mean liquid flow velocity, v, s tends towards a constant, limiting value (Fig. 6). Under this condition the reaction is no longer controlled by mass transport, but entirely by photon flux, and the limiting value relates to the true Faradaic efficiency for a given concentration and describes the extent of interaction between the surface of the photocatalyst and the pollutant molecule, reflecting the ratio between reaction rates of solute and solvent on the catalyst surface [14]. This, however, may depend on concentration if solute adsorption plays a major role. For higher photon fluxes, higher liquid flow rates must be used in order to reach the limiting value of s, i.e. to maintain sufficient supply of electroactive species. A value of 0.0019 M was calculated for s which is similar to kinetic parameters observed for photoelectrocatalytic degradation of AO7 on titanium dioxide electrodes (s = 0.001 M) [13].

The question of stability has not explicitly been addressed in this study. WO_3 is known to be chemically stable in acid electrolytes. So far, operation under light and electrical bias for about 25 h did not lead to visible damage. Further work on this issue is under way.

4. ACKNOWLEDGEMENTS

The authors want to thank Dr. A. Belaidi, *Helmholtz-Zentrum Berlin für Materialen und Energie GmbH*, for preparing and measuring cross sections of samples by scanning electron microscopy. Dr. G. Nauer, *CEST competence center, Austria*, is thanked for the TOC measurements.

REFERENCES

[1] L. Kopp, B. L. Harmon, S. H. Liu, Solid State Commun., 22, 677 (1977).

[2] N. S. Gaikwad, G. Waldner, A. Brüger, A. Belaidi, S.M. Chaqour, M. Neumann-Spallart, J. Electrochem. Soc., 152 (5), G411 (2005).

[3] H. Gerischer in "Solar Energy Conversion – Solid State Physics Aspects", Ed., B. O. Seraphin, Springer, New York 1979.

[4] W. Gissler and R. Memming, J. Electrochem. Soc., 124, 1710 (1977).

[5] M. Pourbaix, "Atlas d'équilibres électrochimiques", Gauthier-Villars et C^{ie}, Paris 1963.

[6] G. Waldner, A. Brüger, N.S. Gaikwad, M. Neumann-Spallart, Chemosphere, 67, 779 (2007).

[7] A. Mills and S. Le Hunte, J. Photochem. Photobiol. A: Chem., 108, 1 (1997).

[8] J. Krýsa, private communication.

[9] D. Monllor-Satoca, L. Borja, A. Rodes, R. Gómez, P. Salvador, Chem. Phys. Chem., 7, 2540 (2006).

[10] S. B. Sadale, S. M. Chaqour, O. Gorochov, M. Neumann-Spallart, Materials Research Bulletin, 43, 1472 (2008).

[11] C. Santato, M. Ulmann, J. Augustynski, J. Phys. Chem. B, 105, 936 (2001).

[12] M. Hepel and S. Hazelton, Electrochim. Acta, 50, 5278 (2005).

[13] P. S. Shinde, P. S. Patil, P. N. Bhosale, A. Brüger, G. Nauer, M. Neumann-Spallart, C. H. Bhosale, Applied Catalysis B: Environmental, 89, 288 (2009).

[14] T. Lana Villarreal, R. Gómez, M. Neumann-Spallart, N. Alonso-Vante, P. Salvador, J. Phys. Chem. B, 108, 15172 (2004).

[15] Powder Diffraction File Alphabetic PDF-2 Data Base, file 43-1035, International Center of Diffraction Data, Newtown Square, PA, USA, 1994.